Mapping the Active Site of CD59

By Jinghua Yu,* Ruben Abagyan,‡ Shanghong Dong,*
Alexander Gilbert,* Victor Nussenzweig,* and Stephen Tomlinson*

*From the *Department of Pathology, New York University Medical Center, New York 10016 and
‡Department of Biochemistry, The Skirball Institute, New York 10016*

Summary

CD59 is a widely distributed membrane-bound inhibitor of the cytolytic membrane attack complex (MAC) of complement. This small (77 amino acid) glycoprotein is a member of the Ly6 superfamily of proteins and is important in protecting host cells from the lytic and proinflammatory activity of the MAC. CD59 functions by binding to C8 and/or C9 in the nascent MAC and interfering with C9 membrane insertion and polymerization. We present data obtained from a combination of molecular modeling and mutagenesis techniques, which together indicate that the active site of CD59 is located in the vicinity of a hydrophobic groove on the face of the molecule opposite to a "hydrophobic strip" suggested earlier. In addition, removal of the single N-linked glycosylation site at Asn18 of CD59 resulted in an enhancement of complement inhibitory activity.

Activation of complement results in the formation of the proteolytic C3/C5 convertases, which can initiate formation of the cytolytic membrane attack complex (MAC)[1]. The MAC is formed by the sequential assembly of the terminal complement proteins C5b, C6, C7, C8, and multiple C9s. Under normal circumstances, complement is activated by, and directed against invading microorganisms. However, under certain circumstances, most notably in some autoimmune and inflammatory conditions, complement can also become deposited on host cells. In addition to causing cell lysis, sublethal concentrations of MAC assembled on host cells mediate various inflammatory processes that can elicit severe pathophysiological effects. Host cell membranes are protected from homologous MAC by CD59, a small glycoprotein attached to the plasma membrane by a glycosylphosphatidylinositol (GPI) anchor. The mature protein consists of 77 amino acids arranged in a single cysteine-rich domain composed of two antiparallel β-sheets, 5 protruding surface loops and a short helix (1, 2). CD59 functions by binding to C8α and/or C9 in the assembling MAC and interfering with C9 membrane insertion and polymerization (3–6).

Several studies have demonstrated the potential usefulness of recombinant soluble complement regulatory proteins for therapy of autoimmune and inflammatory disease (7–11). In addition, MAC-mediated tissue destruction is primarily responsible for hyperacute rejection of porcine organs transplanted into primates, a result of complement activation by natural antibodies (12). CD59 and other complement inhibitors display varying degrees of species selectivity. The expression of human CD59 on transgenic animal organs protects them from human complement-mediated damage and prolongs their survival after transplantation into baboons (13–16). There is thus much interest in the potential use of CD59 and other complement inhibitors, either soluble or expressed on the surface of transgenic pig organs, in human transplantation.

CD59 belongs to the Ly6 superfamily of proteins which includes functional CD59 analogues from other species, snake venom neurotoxins, urokinase-type plasminogen activator receptor and murine Ly6 differentiation antigens (17). Mouse Ly6E antigen (18) is a structural but not functional analogue of CD59 (see Fig. 1). In the approach reported here, functionally important regions of CD59 were determined by replacing regions of Ly6E with corresponding regions from CD59 and assaying expressed chimeric proteins for activity. The active site was then further defined by a series of site-specific mutations, selected as a result of comparing evolutionary conserved residues and modeling of the molecular surface of CD59.

Materials and Methods

Cells and DNA. All DNA manipulations were carried out in the mammalian expression vector pCDNA3 (Invitrogen, San Diego, CA) containing either CD59 or Ly6E cDNA subcloned into its multiple cloning site. pCDNA3 contains a G418 resistance marker. CD59 and Ly6E cDNA were kind gifts from Drs. H. Okada (Nagoya City University, Nagoya, Japan) and U. Hämmerling (Memorial SloanKettering Cancer Center, New York), respectively. Chinese hamster ovary cells (CHO) were used for

---

[1]*Abbreviations used in this paper:* CHO, Chinese hamster ovary cells; GPI, glycosylphosphatidylinositol; MAC, membrane attack complex; NHS, normal human serum.
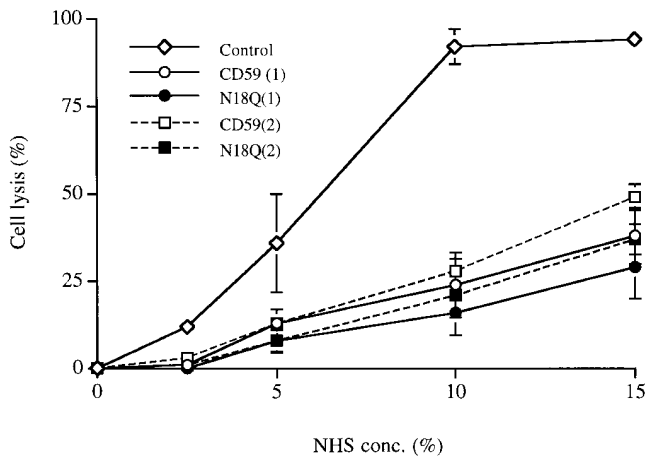
Figure 1. CD59 and Ly6E sequence comparison. Mature protein sequences are shown with the conserved cysteine residues marked (:). The amino acids forming the surface loops and helix of CD59 are shown. The COOH-terminal end of mature Ly6E is predicted.

```
Ly6E
LECYQCYGVPFETSCP-SITCPYPDGVCVTQEAAVIVDSQTRKVKNNLCLP--ICPPNIESMEILGTKVNVKTSCCQEDLCNVAVPN
  :  :    :    :           :              :          :         ::   :
LQCYNCPNP--TADCKTAVNCSSDFDACLITKAG--------LQVYNKCWKFEHCNFNDVTTRLRE--NELTYYCCKKDLCNFNEQLEN
CD59
     loop 1        loop 2         loop 3          loop 4    helix   loop 5    C-terminal peptide
```

protein expression and were maintained in Dulbecco's modified essential medium (DMEM) supplemented with 10% FCS. Stably transfected CHO cell lines were selected after the cultivation of cells in the presence of G418 (GIBCO BRL, Gaithersburg, MD).

Antibodies and Serum. Rabbit antisera to CHO cell membranes, CD59 and to CD59-specific peptide were prepared by standard techniques (19). CHO cell membranes were prepared as described (20). CD59 antigen was prepared from human erythrocytes as described (21). The peptide antigen corresponded to the COOH-terminal sequence of mature CD59 (CKKDLCN-FNEQLE) and was conjugated to KLH for immunization. Peptide synthesis and KLH conjugation was performed by Genemed (South San Francisco, CA). Anti-CD59 peptide Ab was affinity purified by means of peptide immobilized onto CNBr-activated sepharose (Pharmacia, Piscataway, NJ). Anti-CD59 mAbs YTH53.1, MEM43/5, and HC1 were kindly provided by Dr. B.P. Morgan (University of Wales, Cardiff, UK). Each recognize nonoverlapping conformational epitopes on CD59 (22). mAb 2A10 (23) is directed against (NANP)$_n$, a repeat domain of *Plasmodium falciparum* circumsporozoite protein. FITC-conjugated Abs used for flow cytometry were purchased from Sigma Chem. Co. (St. Louis,

MO). Normal human serum (NHS) was obtained from the blood of healthy volunteers in the laboratory and stored at −70°C.

Mutant Construction. Based on the alignment of CD59 and Ly6E amino acid sequences (Fig. 1), cDNA encoding the chimeric constructs depicted in Fig. 2 were prepared. Segments of either CD59 or Ly6E cDNA were generated and joined using PCR. The general procedure used for the generation of chimeric constructs was as described (24). The 5′ and 3′ end primers, which matched an untranslated sequence of either CD59 or Ly6E, included a HindIII and ApaI site, respectively. Using either CD59 or Ly6E cloned into pCDNA3 as template, these primers were paired in a PCR with CD59-Ly6E chimeric primers that spanned the desired crossover point. The PCR products were purified from agarose gel after electrophoresis and used in a second amplification with the primers corresponding to 5′ or 3′ untranslated regions. The resulting full-length CD59-Ly6E chimeric cDNAs were cloned into the HindIII/ApaI sites of pCDNA3 for sequencing and expression. Five site-specific point mutations in CD59 (N18Q, F23D, Y36F, W40Y, and L54N) were prepared by PCR using similar techniques. In the first PCR amplification, 5′ and 3′ primers to CD59 untranslated region were paired with

Figure 2. Diagram of CD59-Ly6E chimeric constructs. All numbers refer to amino acid positions of CD59.

Figure 3. Complement inhibitory activity of unglycosylated CD59. Stable CHO cell clones expressing similar levels of CD59 or unglycosylated CD59 (N18Q) were assayed for their susceptibility to complement. Controls were mock transfected CHO cells. Each point represents the mean of at least four determinations.

primers spanning the target site, and which contained a substituted codon at the target site. An epitope tag was engineered into CD59-Ly6E chimeric proteins between the first and second amino acids of mature CD59. The NH_2-terminal Leu was duplicated at the COOH-terminus of the tag. A 36mer oligonucleotide encoding NANPNANPNA and with appropriate overhangs was inserted at the PstI restriction site of each point-specific mutant, and of CD59 and CD-Ly constructs (chimeras with CD59 at the NH_2 terminus).

CHO Cell Transfection and Selection. pCDNA3 constructs were transfected into CHO cells that were 50–75% confluent. Transfections were carried out with lipofectamine according to the manufacturer's instructions (GIBCO BRL). 3 d after transfection, recombinant protein expression was confirmed, and G418 was added to the medium for selection of stably transfected populations. After 2 wk in selection medium, cells were fluorescently labeled by means of appropriate Abs and sorted by flow cytometry. Stable populations of CHO cells each expressing similar relative levels of recombinant proteins on their surface were isolated by repeated rounds of cell sorting using either the tag-specific mAb 2A10 (for CD59, CD-Ly chimeras, and point mutants) or anti-peptide Ab (for Ly-CD proteins). Three rounds of sorting were usually sufficient to obtain uniform cell populations that were stable for several weeks. Stably transfected CHO cell clones expressing CD59, unglycosylated CD59 and NH_2 terminus tagged CD59 were prepared according to instructions supplied by GIBCO BRL with lipofectamine reagent.

Flow Cytometry. Analysis of cell surface protein expression was performed by flow cytometry using a Beckton Dickinson FACScan®. Detached CHO cells were incubated with appropriate Ab for 30 min at 4°C, washed by centrifugation, incubated with appropriate FITC-conjugated second Ab (30 min/4°C), and washed again before fixation with 2% paraformaldehyde in PBS. All incubations and washing were performed in DMEM/10% FCS. The following Abs and concentrations were used: rabbit anti-COOH-terminal CD59 peptide Ab (30 μg/ml); rabbit anti-CD59 antiserum (1:100); anti-CD59 mAb YTH53.1 IgG (10 μg/ml); anti-tag mAb 2A10 and anti-CD59 mAb MEM 43/5 ascites (1:250); anti-CD59 mAb HC1 culture supernatant (1:25). FITC-conjugated secondary Abs were used between 1:100 and 1:400 final

concentration. Cells for sorting were fluorescently labeled following the procedure above but without fixation. Sorting was done in a Coulter Epics Elite with EPS sort module.

Cell Lysis Assays. Subconfluent CHO cells were detached with versene (GIBCO BRL), washed once and resuspended to 1×10^6/ml in DMEM/10% FCS. An equal volume of calcein-AM (5 μg/ml) (Molecular Probes, Eugene, OR) in DMEM was added and the cells incubated for 15 min at 37°C. The cells were then washed twice, resuspended to their original concentration in DMEM/10% FCS and incubated with rabbit anti-CHO cell membrane antiserum (20% final concentration) for 30 min on ice. The sensitized cells were then centrifuged, resuspended to their original concentration and an equal volume of NHS diluted in DMEM added. After 1 h at 37°C, the cells were centrifuged and cell lysis assessed by measuring released fluorescence in the supernatant. Measurements were performed in microtiter plates using a Labsystems fluoroscan II set to read at excitation 485 nm and emission 538 nm. Cells were lysed with 0.01% saponin for 100% lysis controls. Cell lysis assays were typically performed in 1.5-ml microfuge tubes in a final volume of 200 μl (1×10^5 cells). Cell lysis assays were also performed using propidium iodide, which fluorescently stains dead cells. CHO cells were sensitized to complement as described and 100 μl cells (1×10^6/ml) mixed with NHS dilutions. After 60 min at 37°C, propidium iodide was added (10 μg/ml final) and cell lysis determined by flow cytometry.

Molecular Modeling. A CD59 analytical molecular surface, which is defined as the smooth envelope touching the van der Waals surface of atoms as the solvent probe rolls over the protein molecule, was built with the contour-buildup algorithm (25) as implemented in the ICM program (26). A probe sphere of 1.4 A was used. Molecular models of the point mutants were built and analyzed using the following procedures: (*a*) the structure of CD59 (pdb-code 1cds) solved by NMR (1) was carefully energy minimized; (*b*) appropriate residue modifications introduced; (*c*) the mutated side-chains were energy minimized using the biased probability Monte Carlo sample of the side-chain torsions (27), (*d*) interactions were analyzed by visual inspection using the ICM program.

Results

Role of N-linked Carbohydrate in CD59 Function. Native CD59 is glycosylated at Asn18, and there are conflicting reports concerning its functional importance (28–30). We substituted Asn18 with Gln, and expressed the mutant protein in CHO cells. Fig. 3 shows that CHO cells expressing recombinant wild-type and unglycosylated CD59 are much more resistant to lysis by complement than mock transfected controls. Two stable CHO cell clones expressing unglycosylated CD59 were isolated, and each was matched with a CHO cell clone expressing a similar level of native CD59 for functional assays (Table 1). In both cases, cells expressing unglycosylated CD59 were more resistant to complement than cells expressing similar levels of native CD59. The difference was small but significant ($P < 0.05$) over a range of serum concentrations. The expected reduction in MW of unglycosylated CD59 was confirmed by Western blotting of CHO cell membrane preparations (not shown).

Complement Inhibitory Activity of CD59/Ly6E Chimeric Proteins. To identify regions of CD59 important for function, a series of CD59/Ly6E chimeric proteins containing

Table 1. *Flow Cytometric Analysis of Stable CHO Cell Clones and Sorted CHO Cell Populations Expressing CD59 and Mutant Constructs*

Transfectant	Mean Relative Fluorescence					
	Anti-CD59 polyclonal	Anti-tag mAb 2A10	Anti-CD59 peptide polyclonal	Anti-CD59 mAb YTH53.1	Anti-CD59 mAb MEM43/5	Anti-CD59 mAb HC1
CD59	1246	–	–	1218	–	–
CD59-tagged	1207	695	–	1119	–	–
CD59 (1)	1314	–	–	1299	–	–
N18Q (1)	1196	–	–	1201	–	–
CD59 (2)	–			289	–	–
N18Q (2)	–			221	–	–
CD59 (CD-Ly set)	–	820	–	–	–	–
CD-Ly 24	–	1220	–	–	–	–
CD-Ly 47	–	894	–	–	–	–
CD-Ly 57	–	798	–	–	–	–
CD-Ly 64	–	980	–	–	–	–
CD59 (Ly-CD set)	–	–	632	–	–	–
Ly-CD 16	–	–	561	–	–	–
Ly-CD 31	–	–	516	–	–	–
Ly-CD 39	–	–	616	–	–	–
CD59 (1)	–	986	–	766	460	826
CD59 (F23D)	–	780	–	727	448	770
CD59 (Y36F)	–	812	–	686	404	770
CD59 (2)	–	305	–	480	242	434
CD59 (L54N)	–	240	–	316	165	376
CD59 (W40Y)	23	–	–	12	–	–

Mean relative fluorescence of mock transfected CHO cells was below 20 with all Abs. Figures are relative within each grouped set.

either CD59 or Ly6E at their NH_2-terminus were expressed on CHO cells. We reasoned that the residues involved in ligand binding were probably located in surface loops. For this reason, most of the chosen switch over points between CD59 and Ly6E were at selected loop boundaries (see Fig. 2).

CHO cell populations expressing similar levels of recombinant CD59 or chimeric proteins were assayed for their susceptibility to human complement. The functional data obtained with the CD-Ly chimeras (CD59 at NH_2 terminus) revealed that the region of CD59 which lies COOH-terminal to residue 57 is not required for function; both CD-Ly 57 and CD-Ly 64 possessed the same specific activity as wild type CD59 (Fig. 4). The other CD-Ly chimeras which contained shorter CD59-specific sequences had no complement inhibitory activity. Of the Ly-CD chimeras (Ly6E at NH_2 terminus), only Ly-CD 16 possessed any functional activity (Fig. 4). The specific activity of Ly-CD

16 was ~85% that of wild-type CD59. Taken together, these data indicate that the functionally important region of CD59 is located between amino acids 16 and 57 in the primary structure.

To quantitate the relative surface expression of CD59 and CD-Ly chimeric proteins, a 10–amino acid epitope tag was engineered onto the NH_2 termini of the constructs. The tag did not affect the expression (Table 1) or the function (Fig. 5) of CD59. However, when the tag was placed at the NH_2 terminus of Ly6E in the Ly-CD constructs, it interfered with expression and function of the chimeras. Therefore, surface expression of Ly-CD chimeras was quantitated using a rabbit Ab against a peptide corresponding to a sequence from the COOH terminus of CD59 (Table 1). This Ab reacted quantitatively with CHO cell clones stably expressing different levels of CD59 (not shown). Cell populations used in these experiments were obtained by several rounds of cell sorting, and separate CD-Ly and Ly-
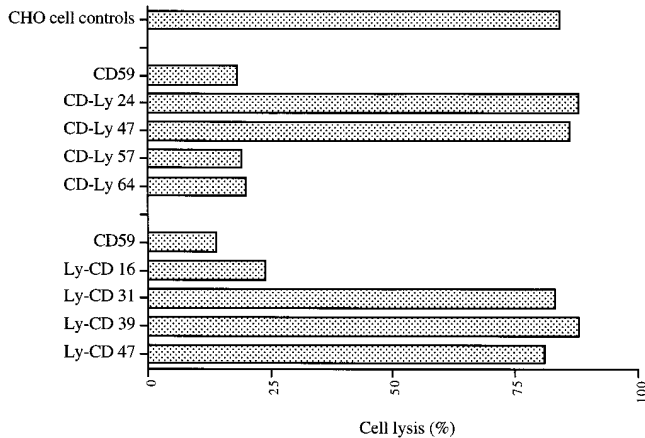
Figure 4. Complement resistance of CHO cells expressing CD59 and CD59-Ly6E chimeric proteins. Complement resistance of CHO cell populations expressing similar levels of either CD59-Ly6E or Ly6E-CD59 chimeras was compared to cells expressing similar levels of CD59. Cells were exposed to 10% NHS. Depending on whether the chimeric protein contained CD59 at its NH₂ or COOH terminus, different methods were used to quantitate relative expression. Therefore activity of chimeras should be compared to CD59 activity within each set.

Figure 5. Complement inhibitory activity of epitope tagged and untagged CD59. Stable CHO cell clones expressing similar levels of CD59 or CD59 containing an NH₂-terminal peptide tag (NANPNANPNA), were assayed for their susceptibility to complement. Expression was quantitated using anti-CD59 mAb YTH53.1 and rabbit anti-CD59 Ab.

CD sets were prepared, each with a corresponding CHO cell population expressing a similar level of CD59.

Modeling the Molecular Surface of CD59. To reveal the hypothetical location and extent of the functional site, we built a model of the molecular surface of CD59 and analyzed: (*a*) the three-dimensional location of the fragments that can be replaced by the Ly6E fragments, (*b*) the distribution of surface patches that are conserved between CD59 of seven different species that are either closely related to human, or that have been shown to inhibit human complement (Fig. 6), and finally, (*c*) the surface shape. A very clear picture emerged from this analysis. Fig. 7 *a* displays the molecule in an orientation that shows that the regions of CD59 that can be replaced by Ly6E without loss of function (1-16 and 57-77) are located at the backside of the molecule (in yellow, Fig. 7 *a*). From the position of residue 77, to which the GPI membrane anchor is attached, it can be predicted that the active site is located on the exposed face of the molecule.

Comparison of CD59 sequences within the region required for function (residues 16-57, Fig. 6) reveal a number of evolutionary conserved residues (Fig. 6). However, of these residues, only five are located on the surface of the shown face of the molecule, and three (Y36, W40, and L54) are conspicuously grouped together in a deep groove (Fig. 7 *b*, conserved residues colored green). Furthermore, conserved residue classes (Fig. 7 *b*, colored blue) are located above and below the conserved residues within this groove. From top to bottom these residue positions are (refer to Fig. 7 *b*): no. 31: Ala or Ser, a small residue, presumably important to keep the hypothetical binding groove open; no. 59: Leu or Val, a hydrophobic residue, outside the CD59 16-57 sequence, but conserved in Ly6E; no. 36: Tyr, no. 54 Leu and no. 40 Trp, conserved residues; no. 23: Phe or Leu, a hydrophobic residue, and no. 41: Lys or
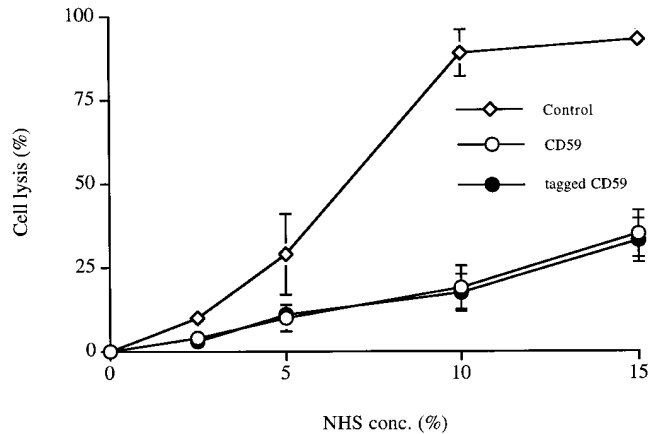
Arg, the only charged residues. The only addition to this list of conserved residues at the shown face of the molecule are Val 35 and two conserved Cys-Cys bridges (Cys19-Cys39, and Cys6-Cys13, shown in yellow). Val 35 and Cys6-Cys13 are located at the inner surface of a tunnel, an interesting structural feature of the molecule (these residues are obscured by the tunnel in Fig. 7 *b*). The conserved cysteines are most likely necessary for conservation of the topology of the molecule.

Effect of Point Mutations within the Predicted Functional Site of CD59. The three conserved residues (shown in green, Fig. 7 *b*) and the conserved hydrophobic residue at position F23 within the putatively identified binding groove of CD59 were individually targeted for site-specific mutagen-

```
            1        10        20        30
Human      LQCYNCPNPTADCKTA VNCSSDFDACLITKAGLQVYNKC
Baboon     LQCYNCPNPTTNCKTA INCSSGFDTCLIARAGLQVYNQC
Marmoset   LQCYSCPYSTARCTTT TNCTSNLDSCLIAKAGLRVYYRC
Af.gr.mon  LQCYNCPNPTTDCKTA INCSSGFDTCLIARAGLQVYNQC
Owl mon    LQCYSCPYPTTQCTMT TNCTSNLDSCLIAKAGSRVYYRC
Rat        LRCYNCLDPVSSCKTN STCCSPNLDACLVAVSGKQVYQQC
H.Saimiri  LQCYNCSHSTMQCTTS TSCTSNLDSCLIAKAGSGVYYRC


            40        50        60        70
Human      WKFEHCNFNDVTTRLREN ELTYYCCKKDLCNFNEQLEN
Baboon     WKFANCNFNDISTLLKES ELQYFCCKEDLCNEQLENGG
Marmoset   WKFEDCTFRQLSNQLSEN ELKYHCCRENLCNFNGILEN
Af.gr.mon  WKFANCNFNDISTLLKES ELQYFCCKKDLCNFNEQLEN
Owl mon    WKFEDCTFSRVSNQLSEN ELKYYCCKKNLCNFNEALKN
Rat        WRFSDCNAKFILSRLEIA NVQYRCCQADLCNKSFEDKPNNG
H.Saimiri  WKFDDCSFKRISNQLSET QLKYHCCKKNLCNVNKGIENIKRTIS
```

Figure 6. Amino acid sequence alignment of CD59 and CD59 homologues from different species. The conserved residues located in the groove that are shown in green in Fig. 7 *b* are in bold, and conserved residue classes shown in blue in Fig. 7 *b* are underlined. Residues 16-57 are shown in plain text. Note that not all of the conserved residues indicated above occur on the shown surface of the molecule displayed in Fig. 7 *b*. The sequences that can be replaced by Ly6E, and which are therefore not required for function are in italics. Sequences shown are human CD59 (39) and homologues from Baboon (40), Marmoset (41) (GenBank acc. no. L22860). African green monkey (40), Owl monkey (41) (GenBank accession no. L22861), Rat (42), and Herpes Saimiri virus (43).
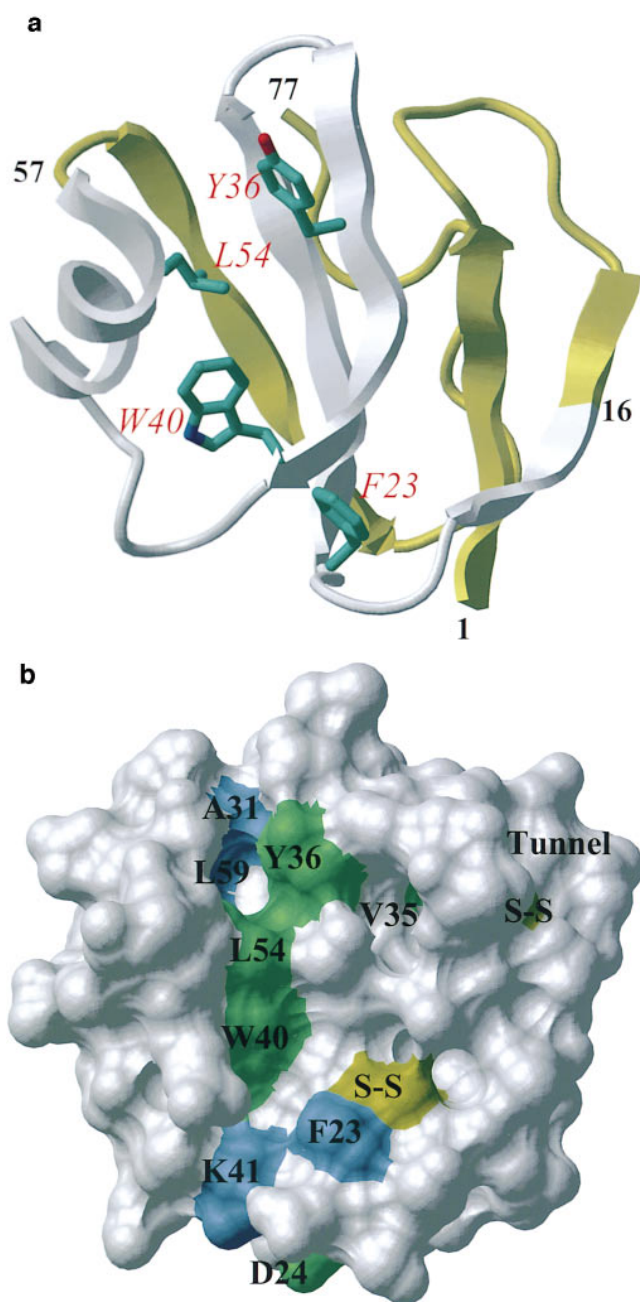
Figure 7. Diagram of CD59. (*a*) Ribbon diagram (1). Conserved residues (Tyr36, Trp40, and Leu54) and Phe23 (always hydrophobic) which were mutated for functional studies are shown. The two fragments of the protein (1–16 and 57–77) that can be replaced with Ly6E sequence without affecting function are shown by yellow ribbon. (*b*) Molecular surface of CD59. The exposed surface patches of all of the evolutionary conserved residues that occur between positions 16–57 on the displayed face of the molecules are shown (green patches). Conserved residue classes are shown in blue (refer to text for details). The colored patches represent the molecular surface of the side chains of conserved residues and residue classes.

esis. The four mutant CD59s prepared were F23D (Phe at position 23 changed to Asp), Y36F, W40Y and L54N. The amino acids used for the substitutions were chosen to have similar shape but different physico-chemical properties.

The W40Y mutant was not stably expressed on the surface of transfected CHO cells. Of the three expressed mutant proteins, L54N had almost no function, F23D retained some but significantly reduced function, and Y36F had normal function (Fig. 8). For unknown reasons, only relatively moderate levels of the L54N mutant protein could be expressed on CHO cells, but activity was compared with CHO cells expressing similar levels of wild-type CD59 (see Table 1). In an attempt to assess whether the mutant proteins were correctly folded, we studied their reactivity with three different mAbs that each bind to non-overlapping conformational epitopes on CD59. All mutant proteins were recognized by these antibodies (Table 1).

Discussion

The results in this report represent a first approximation at defining the active site of CD59. We have shown that: (*a*) glycosylation of CD59 at Asn18 is not required for function; (*b*) replacement of CD59 sequences 1–16 and 57–77 with those of non-functional Ly6E did not affect CD59 activity. These regions are therefore not required for CD59 activity, and they map to the backside of the molecule that is closer to the cell surface (Fig. 7 *a*); (*c*) a comparison of sequences of human CD59 and CD59 homologues from other species within the identified functional region (amino acids 16–57), reveal an almost linear arrangement of conserved residues and residue classes in the three dimensional structure. These residues were predominantly hydrophobic in character, and were not contiguous in the primary structure. Together they marked a groove across the molecule (Fig. 7 *b*); (*d*) mutation of residues within this groove disrupted the function of the expressed mutant proteins.

Taken together, these data indicate that the active site of CD59 is on the front (facing away from membrane) face of the molecule and involves residues located along a hydrophobic groove defined by evolutionary conserved residues. In further support of this conclusion, it was recently shown that a correctly folded W40E mutant (residue located within hydrophobic groove, Fig. 7 *b*) expressed on the surface of CHO cells was inactive (Rushmere, N.K., D.L. Bodian, S.J. Davis, S. Tomlinson, and B.P. Morgan. 1996. XVIth International Complement Workshop. Boston, MA). In a previous report, Kieffer et al. (2) suggested that a relatively hydrophobic strip composed of exposed Tyr and Phe residues may constitute the functional site of CD59. Of note however, these residues are located on the opposite face and perpendicular to the hydrophobic groove identified in this report.

All but one of the Ly-CD and CD-Ly chimeric proteins expressed on CHO cells possessed either full or zero activity, making interpretation of data simple. The Ly-CD 16 chimera displayed slightly less (∼15%) activity than wild type CD59. The simplest explanation for this, taking into account the modeling and point mutation data, is that the NH₂-terminal sequence of Ly6E causes a change in the tertiary conformation of the active site of CD59. We cannot
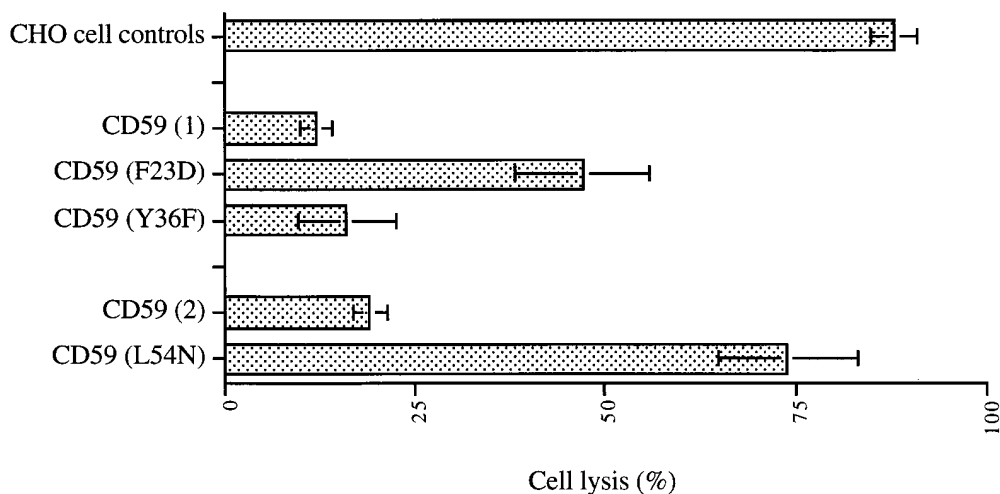
Figure 8. Complement resistance of CHO cells expressing CD59 and site-specific CD59 mutants. Complement resistance of CHO cell populations expressing similar levels of either CD59 or CD59 containing the indicated amino acid substitutions was determined. Cells were exposed to 10% NHS.

exclude however, that the NH_2-terminal sequence of CD59 may contribute to its activity.

The rationale in choosing the substituted residues in the CD59 point mutants was as follows: (*a*) F23D. Aspartate is smaller than phenylalanine, but has a consistent shape with branching at Cγ carbon; (*b*) Y36F. Phenylalanine is lacking the hydroxyl group of tyrosine, and based on its conservation, this group may be important; (*c*) W40Y. Tyrosine is smaller than tryptophane and the aromatic ring superimposes well onto the first ring of tryptophane; (*d*) L54N. Asparagine is very close to leucine in shape and both side-chains branch at Cγ, although the arrangement at Cγ is tetrahedral for leucine and flat for asparagine. Of the four point mutants prepared, one (Y36F) retained function, two (F23D and L54N) disrupted function but preserved protein topology, and one (W40Y) could not be stably expressed. By building an explicit model of this mutant we found that mutation of Trp40 to Tyr40 leads to a severe clash of the hydroxyl group with the backbone H alpha atom of Val50. This clash cannot easily be resolved and likely leads to the loss of tertiary structure. The near full functional activity of Y36F suggests either that this residue is not involved in ligand binding, or that ligand interaction is primarily with the phenol ring, rather than hydrogen bonding via the hydroxyl group. A further series of multiple residue mutations within and around the hydrophobic groove will better define the active site.

It is not clear what function the N-linked carbohydrate of CD59 may serve. It may be necessary for costimulation of T cell activation (31, 32); it has been reported that the ability of CD59 to enhance CD58-dependent T cell responses is dependent on the N-linked carbohydrate (33). Earlier reports are in conflict over the requirement of N-linked glycosylation for CD59 complement inhibitory function (28–30). Here we confirm that glycosylation at Asn18 is not required for the inhibition of C5b-9 assembly on the cell surface. In fact, the absence of the carbohydrate enhances slightly, but significantly, the complement inhibitory activity of the protein. The mechanism for this increase in inhibitory activity is not clear, but it is intriguing that mem-

brane sialic acid has recently been described as an acceptor for C5b6, thus enhancing C5b-9–mediated lysis (34). The absence of the sialylated carbohydrate of CD59 may therefore decrease, in a non-specific manner, C5b6 binding to the cell surface. Whatever the mechanisms involved, our data indicate that CD59 lacking N-linked carbohydrate yields an improved inhibitor, an important consideration in designing complement inhibitors for therapeutic applications and in engineering animal organs for human transplantation.

CD59 interferes with the final stages of MAC assembly either by binding to the α-chain of C8 in C5b-8 and blocking the binding of C9, by binding to C9 in the nascent C5b-9 complex and preventing proper membrane insertion and C9 polymerization, or by both mechanisms (3, 5, 6). If both mechanisms are operative, then the identification of a single functionally important site in CD59 would suggest that both C8α and C9 bind at this site. The putative CD59 binding site lies in the vicinity of a deep extended linear and hydrophobic groove. These characteristics are consistent with the ligand being an unfolded polypeptide chain with exposed hydrophobic residues, as is postulated to occur when C8 and C9 interact to form the MAC. Of possible relevance, the molecular surface contains a long tunnel under loop Asn8 to Cys13. There are two side chains facing the inner surface of the tunnel, the conserved Val35 as well as residues Asn, Ser, or Gln at position 72. This channel may represent a secondary binding site, but one that may not be required for its complement inhibitory function.

The intense current interest in inhibitors of complement is due to their potential use as anti-inflammatory agents and for preventing unwanted complement-mediated cytolysis. In addition to its role in hyperacute rejection of xenografts, there is evidence indicating that complement-mediated cytolysis is important in the pathogenesis of many autoimmune and inflammatory diseases (35). Understanding precisely how CD59 and other complement inhibitors function will provide a foundation for designing functional inhibitors, possibly multivalent and with enhanced inhibitory activity. The identification of the active site for CD59 may also en-

able the design of CD59 inhibitors, quite possibly with affinities higher than those of its natural ligands (36); CD59 and other membrane-bound inhibitors of complement are functionally expressed on tumor cells (37, 38), and inhibiting CD59 on tumor cells may enhance their lysis when targeted by complement activating tumor-specific antibodies.

References

1. Fletcher, C.M., R.A. Harrison, P.J. Lachmann, and D. Neuhaus. 1994. Structure of a soluble, glycosylated form of the human complement regulatory protein CD59. *Structure.* 2: 185–199.
2. Kieffer, B., P.C. Driscoll, I.D. Campbell, A.C. Willis, P.A. van der Merwe, and S.J. Davis. 1994. Three-dimensional solution structure of the extracellular region of the complement regulatory protein CD59, a new cell-surface protein domain related to snake venom neurotoxins. *Biochem.* 33:4471–4482.
3. Rollins, S.A., J.I. Zhao, H. Ninomiya, and P.J. Sims. 1991. Inhibition of homologous complement by CD59 is mediated by a species-selective recognition conferred through binding to C8 within C5b-8 or C9 within C5b-9. *J. Immunol.* 146: 2345–2351.
4. Ninomiya, H., and P.J. Sims. 1992. The human complement regulatory protein CD59 binds to the alpha chain of C8 and to the "b" domain of C9. *J. Biol. Chem.* 267:13675–13680.
5. Rollins, S.A., and P.J. Sims. 1990. The complement-inhibitory activity of CD59 resides in its capacity to block incorporation of C9 into membrane C5b-9. *J. Immunol.* 144:3478–3483.
6. Meri, S., B.P. Morgan, A. Davies, R.H. Daniels, M.G. Olavesen, H. Waldemann, and P.J. Lachmann. 1990. Human protectin (CD59), an 18-20 kD complement lysis restricting factor, inhibits C5b-8 catalysed insertion of C9 into lipid bilayers. *Immunol.* 72:1–9.
7. Weisman, H.F., T. Bartow, M.K. Leppo, H.C. Marsh, G.R. Carson, M.F. Consino, M.P. Boyle, K.H. Roux, M.L. Weisfeldt, and D.T. Fearon. 1990. Soluble human complement receptor type 1: in vivo inhibitor of complement suppressing post-ischemic myocardial inflammation and necrosis. *Science (Wash. DC).* 249:146–151.
8. Moran, P., H. Beasly, A. Gorrel, E. Martin, P. Gribling, H. Fuchs, N. Gillet, L.E. Burton, and I.W. Caras. 1992. Human recombinant soluble decay accelerating factor inhibits complement activation *in vitro* and *in vivo. J. Immunol.* 149:1736–1743.
9. Christiansen, D., J. Milland, B.R. Thorley, I.F. McKenzie, and B.E. Loveland. 1996. A functional analysis of recombinant soluble CD46 in vivo and a comparison with recombinant soluble forms of CD55 and CD35 in vitro. *Eur. J. Immunol.* 26:578–585.
10. Sugita, Y., K. Ito, K. Shiozuka, H. Gushima, M. Tomita, and Y. Masuho. 1994. Recombinant soluble CD59 inhibits reactive haemolysis with complement. *Immunol.* 82:34–41.
11. Matis, L.A., and S.A. Rollins. 1995. Complement-specific antibodies: Designing novel anti-inflammatories. *Nat. Med.* 1: 839–842.
12. Parker, W., D. Bruno, and J.L. Platt. 1995. Xenoreactive natural antibodies in the world of natural antibodies: typical or unique? *Transplant Immunol.* 3:181–191.
13. McCurry, K.R., D.L. Kooyman, C.G. Alvarado, A.H. Cotterell, M.J. Martin, J.S. Logan, and J.L. Platt. 1995. Human complement regulatory proteins protect swine-to-primate cardiac xenographs from humoral injury. *Nature Med.* 1:423–427.
14. Roush, W. 1995. New ways to avoid organ rejection buoys hopes. *Science (Wash. DC).* 270:234–235.
15. Fodor, W.L., B.L. Williams, L.A. Matis, J.A. Madri, S.A. Rollins, J.W. Knight, W. Velander, and S.P. Squinto. 1994. Expression of a functional human complement inhibitor in a transgenic pig as a model for the prevention of xenogeneic hyperacute organ transplantation. *Proc. Natl. Acad. Sci. USA.* 91:11153–11157.
16. Byrne, G.W., K.R. McCurry, D. Kagan, C. Quinn, M.J. Martin, J.L. Platt, and J.S. Logan. 1995. Protection of xenogeneic cardiac endothelium from human complement by expression of CD59 or DAF in transgenic mice. *Transplantation.* 60:1149–1156.
17. Ploug, M., and V. Ellis. 1994. Structure-function relationships in the receptor for urokinase-type plasminogen activator. Comparison to other members of the Ly-6 family and snake venom alpha-neurotoxins. *FEBS Lett.* 349:163–168.
18. LeClair, K.P., R.G. Palfree, P.M. Flood, U. Haemmerling, and A. Bothwell. 1986. Isolation of a murine Ly-6 cDNA reveals a new multigene family. *EMBO (Eur. Mol. Biol. Organ.) J.* 5:3227–3234.
19. Harlow, E., and D. Lane. 1988. Antibodies. A laboratory manual. Cold Spring Harbor Laboratory, Cold Spring Harbor, New York. 53–138.
20. Diaz, R., L. Mayorga, and P. Stahl. 1988. In vitro fusion of endosomes following receptor-mediated endocytosis. *J. Biol. Chem.* 263:6093–6100.

21. Okada, R., N. Okada, T. Fujita, and H. Okada. 1990. Purification of 1F5 antigen that prevents complement attack on homologous cell membranes. *J. Immunol.* 144:1823–1827.

22. Bodian, D.L., S.J. Davies, B.P. Morgan, and N.K. Rushmere. 1997. Mutational analysis of the active site and antibody epitopes of the complement-inhibitory glycoprotein, CD59. *J. Exp. Med.* In Press.

23. Nardin, E.H., V. Nussenzweig, and R.S. Nussenzweig. 1982. Circumsporozoite proteins of human malaria parasites *Plasmodium falciparum* and *Plasmodium vivax. J. Exp. Med.* 156:20–30.

24. Vallejo, A.N., R.J. Pogulis, and L.R. Pease. 1995. PCR Primer. A Laboratory Manual. Cold Spring Harbor Laboratory Press, Cold Spring Harbor, NY. 603–612.

25. Totrov, M.M., and R.A. Abagyan. 1996. The contour-buildup algorithm to calculate the analytical molecular surface. *J. Struct. Biol.* 116:138–143.

26. Molsoft, L.C.C. 1996. ICM software manual version 2.5.

27. Abagyan, R.A., and M.M. Totrov. 1994. Biased probability Monte Carlo conformational searches and electrostatic calculations for peptides and proteins. *J. Mol. Biol.* 235:983–1002.

28. Nakano, Y., K. Noda, T. Endo, A. Kobata, and M. Tomita. 1994. Structural study on the glycosyl-phosphatidylinositol anchor and the asparagine-linked sugar chain of a soluble form of CD59 in human urine. *Arch. Biochem. Biophys.* 311: 117–126.

29. Ninomiya, H., B.H. Stewart, S.A. Rollins, J. Zhao, A.L. Bothwell, and P.J. Sims. 1992. Contribution of N-linked carbohydrate of erythrocyte antigen CD59 to its complement-inhibitory activity. *J. Biol. Chem.* 267:8404–8410.

30. Akami, T., K. Arakawa, M. Okamoto, I. Fujiwara, I. Nakai, M. Mitsuo, R. Sawada, M. Naruto, and T. Oka. 1994. Enhancement of the complement regulatory function of CD59 by site-directed mutagenesis at the N-glycosylation site. *Transp. Proc.* 26:1256–1258.

31. Hahn, W.C., E. Menu, A.L. Bothwell, P.J. Sims, and B.E. Bierer. 1992. Overlapping but nonidentical binding sites on CD2 for CD58 and a second ligand CD59. *Science (Wash. DC).* 256:1805–1807.

32. Deckert, M., J. Kubar, D. Zoccola, G. Bernard-Pomier, P. Angelisova, V. Horejsi, and A. Bernard. 1992. CD59 molecule: a second ligand for CD2 in T cell adhesion. *Eur. J. Immunol.* 22:2943–2947.

33. Menu, E., B.C. Tsai, A.L.M. Bothwell, P.J. Sims, and B.E. Bierer. 1994. CD59 costimulation of T cell activation. *J. Immunol.* 153:2444–2456.

34. Marshall, P.M., A. Hasegawa, E.A. Davidson, V. Nussenzweig, and M. Whitlow. 1996. Interaction between complement proteins C5b-7 and erythrocyte membrane sialic acid. *J. Exp. Med.* 184:1225–1232.

35. Complement in Health and Disease. 1993. K. Whaley, M. Loos, and J.M. Weiter, editors. Kluwer Academic Publishers, Dordrecht, Germany.

36. Verlinde, C.L., and W.G. Hol. 1994. Structure-based drug design:progress, results and challenges. *Structure.* 2:577–587.

37. Hakulinen, J., and S. Meri. 1994. Expression and function of the complement membrane attack complex inhibitor protectin (CD59) on human breast cancer cells. *Lab. Invest.* 71: 820–827.

38. Junnikkala, S., J. Hakulinen, and S. Meri. 1994. Targeted neutralization of the complement membrane attack complex inhibitor CD59 on the surface of human melanoma cells. *Eur. J. Immunol.* 24:611–615.

39. Sugita, Y., T. Tobe, E. Oda, M. Tomita, K. Yasukawa, N. Yamaji, T. Takemoto, K. Furuichi, M. Takayama, and S. Yano. 1989. Molecular cloning and characterization of MACIF, an inhibitor of membrane channel formation of complement. *J. Biochem.* 106:555–557.

40. Fodor, W.L., S.A. Rollins, S. Bianco-Caron, W.V. Burton, E.R. Guilmette, R.P. Rother, G.B. Zavoico, and S.P. Squinto. 1995. Primate terminal complement inhibitor homologues of human CD59. *Immunogen.* 41:51.

41. Rother, R.P., S.A. Rollins, J. Menone, W.L. Fodor, and S.P. Squinto. 1993. Marmoset and Owl monkey. (unpublished) Entrez report: ATRCD59H, accession L22860.

42. Rushmere, N.K., R.A. Harrison, C.W. van der Berg, and B.P. Morgan. 1994. Molecular cloning of the rat analogue of human CD59: structural comparison with human CD59 and identification of a putative active site. *Biochem. J.* 304:595–601.

43. Albrecht, J.C., J. Nicholas, K.R. Cameron, C. Newman, B. Fleckenstein, and R.W. Honess. 1992. Herpesvirus saimiri has a gene specifying a homologue of the cellular membrane glycoprotein CD59. *Virol.* 190:527–530.